LA-UR-23-31601

Approved for public release; distribution is unlimited.

Title:	Niowave Neutron Source Converter: Lead-Bismuth-Eutectic (LBE) Windowless Target Design and Evaluation
Author(s):	Singh, Bhavini Seong, Jee Hyun Olivas, Eric Richard Woloshun, Keith Albert
Intended for:	Report
Issued:	2023-10-10

Niowave Neutron Source Converter

Lead-Bismuth-Eutectic (LBE) Windowless Target Design and Evaluation

In Partial Fulfillment of the Deliverable Requirements for Niowave LANW-A6 Support by LANL

Jee Hyun Seong
Bhavini Singh
Eric R. Olivas
Keith A. Woloshun

LA-UR-23-xxxxx
23-10-10

Los Alamos NATIONAL LABORATORY

Prepared for: U.S. Department of Energy/National Nuclear Security Administration, Los Alamos Field Office

Contents

Figures

Tables

Acronyms and Abbreviations

Acronym	Definition
CAD	Computer adided design
CFD	Computational fluid dynamics
CHT	Conjugate heat transfer
CSG	Constructive solid geometry
HTC	Heat transfer coefficient
LBE	Lead-bismuth-eutetic
LANL	Los alamos national laboratory
MCNP	Monte carlo N-particle
NNSA	National nuclear security admnistration
SS	Stainless-steel
UM	Unstructured mesh

EXECUTIVE SUMMARY

Los Alamos National Laboratory (LANL) is working with Niowave on the design and evaluation of their lead-bismuth-eutectic (LBE) windowless target (i.e., neutron source converter). Niowave plans to use 200 kW electron beam at 40 MeV beam energy to produce neutrons by photonuclear reaction with LBE. Then, the neutrons undergo fission at the surrounding uranium target assembly (UTA) to produce Molybdenum-99 (Mo-99) as a fission product, which eventually decays to Technetium-99 (Tc-99m). Tc-99m is one of important radioisotopes that is used for medical diagnostics. LANL conducted 3D multiphysics analysis for the Niowave neutron converter design and provided design assessment in thermohydraulic aspects. LANL conducted radiation transport calculations using Monte-Carlo N-Particle (MCNP) code with unstructured meshing scheme. The 3D volumetric heating profiles in the LBE and Stainless-Steel (SS) housing were imported into multiphase computational fluid dynamics (CFD) to obtain 3D temperature profiles of LBE and SS through conjugate heat transfer (CHT) analysis. The key findings are:

- LBE film thickness at the center of the beam is approximately 1.6 cm with a maximum LBE velocity of approximately 1.8 m/s, which is below a 2 m/s limit to avoid erosion issues on supporting structures.

- Heat deposition in the LBE peaks at ~1 cm depth from the LBE free-surface because of the forward interactions of electron, photon, and neutron with LBE.

- LBE maximum temperature is ~360 ℃, which is below LBE evaporation initiative temperature, ~450 ℃.

- LBE-SS interface temperature is ~350 ℃, which is below the safety thermal limit to prevent severe corrosion on SS.

The results indicate that Niowave's neutron converter design satisfies both hydraulic and thermal criteria for safe operation. By virtue of such computational analysis, Niowave can move toward establishing an experimental setup to experimentally test their LBE neutron converter. The following sections describe the detailed work done by LANL.

1 Introduction

Los Alamos National Laboratory (LANL) supported Niowave Inc. as a part of the National Nuclear Security Administration (NNSA)'s Molybdenum-99 program. LANL helped Niowave develop, design, and evaluate a lead-bismuth-eutectic (LBE) windowless target used to produce neutrons (so-called neutron converter) by electron irradiation at a beam power of 200 kW with a beam energy of 40 MeV and beam current of 5 mA. Two superconducting electron accelerators are used to irradiate two neutron source converters embedded in an uranium target assembly (UTA), as shown in Fig. 1. The neutron converter is designed such that there is a thin stainless steel (SS) housing surrounding LBE flow in vacuum. The LBE layer falls, driven by gravity, and forms free-surface in vacuum. The heat deposited on the irradiated LBE target and SS housing is removed through forced convection by LBE flow. As an extension to Niowave's 1D/2D analyses, LANL provided 3D simulation and multiphysics analysis capabilities. This report builds on prior work by LANL on the design and analysis of the Niowave 200 kW converter [1] presenting computational fluid dynamics (CFD) analysis coupled with Monte Carlo N-Particle (MCNP) radiation transport calculations for the converter system.

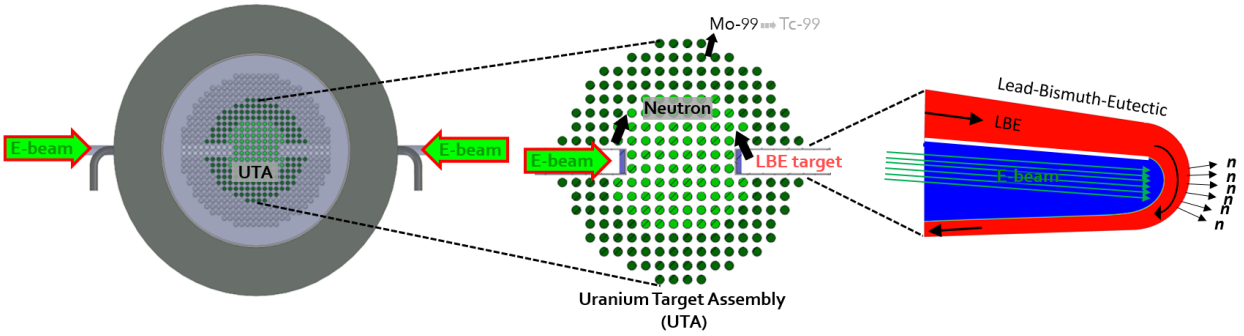

Figure 1. Niowave UTA and neutron source converter concept *(Images created by Niowave)*.

2 2D/3D Hydraulic simulations for design optimization

A LBE neutron source converter was designed to accommodate an electron beam size of 5cm×5cm. The design was optimized by changing design parameters, as shown in Fig. 2, where t_0 is the height of inlet channel, α is the angle of inlet slope, R_1 is the curvature of upper corner, L is the length of the region of flow where the LBE is free falling downward toward the bottom of the channel, β is the angle of the downward falling slope, R_2 is the curvature of lower corner, and γ is the angle of the outlet slope. Three guidelines were suggested for hydraulics analysis:

A. LBE flow thickness at the electron beam path is advised to be as thick as possible. A thicker LBE layer would benefit neutron production as well as lessen thermal load on SS wall.

B. LBE maximum velocity should be lower than 2 m/s to prevent etching and erosion problems at the LBE-SS interface due to heavy liquid metal flow.

C. LBE pressure should be positive to avoid cavitation of LBE flow which is adjacent to ultra-high vacuum.

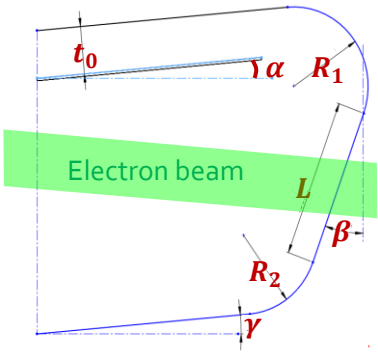

Figure 2. LBE neutron source converter design parameters.

Table 1 summarizes user-defined settings for the ANSYS Fluent multiphase simulation. Nitrogen from the Fluent Database was used as a secondary fluid to replicate vacuum conditions. Fig. 3 shows imported LBE properties and Fig. 4 shows imported SS properties as a function of temperature.

Table 1. User-defined settings for the ANSYS Fluent multiphase simulation.

Material Properties				
	Density	Specific heat	Thermal conductivity	Viscosity
LBE	Piecewise-linear (see Fig. 3)			
SS	7771 [kg/m^3]	Piecewise-linear (see Fig. 4)		-
General Settings				
Solver	Pressure-based, Steady			
Operating Conditions	Pressure 1 Pa, Gravity acceleration 9.8 m/s^2			
Viscous Model				
Turbulent Model	Reynolds Averaged Navier Stokes (RANS), Standard k-epsilon			
Near-Wall Treatment	Enhanced wall treatment			
Multiphase Model				
Eulerian Model	Homogeneous volume of fluid, Implicit			
Phase Interaction	Surface tension force modeling, Surface tension coefficient with 0.41 N/m			
Boundary Conditions				
Inlet	Velocity magnitue 0.534 m/s, Temperature 200 ℃, LBE volume fraction 1.			
Outlet	Gauge pressure 0 Pa, Backflow total temperature 200 ℃.			

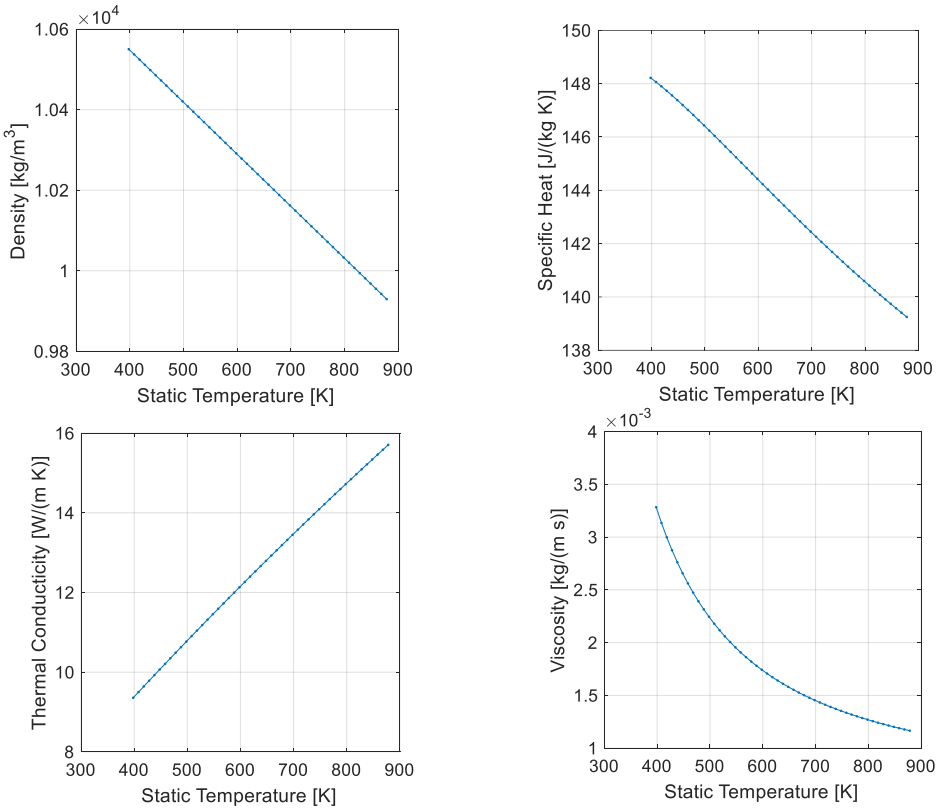

Figure 3. LBE properties as a function of static temperature.

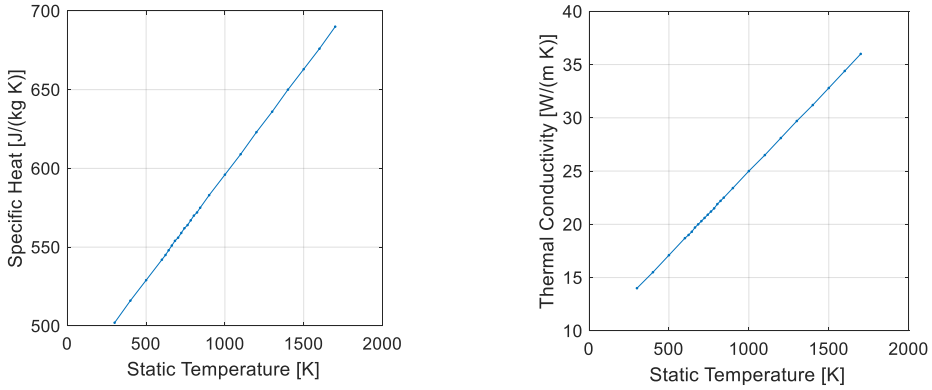

Figure 4. SS properties as a function of static temperature.

Evaluation of design parameters for 7 cases was conducted, as tabulated in Table 2. Fig. 5 shows LBE pressure distribution for case 1, case 3, and case 7, which demonstrates the effect of inlet slope on pressure. The colorbar is constrained to show positive pressure region-only since negative pressure is unrealistic and simply indicates potential cavitation occurrence. An upslope-inlet design was suggested to maintain a favorable pressure gradient (i.e., positive pressure at the inlet channel). In Table 2, case 2 and case 4 indicate that a larger inlet channel height reduces LBE maximum velocity and increases LBE film thickness, based on which an inlet channel height of 4 cm was advised. Case 4, Case 5, and Case 6 show that a rounded back wall design gives lower maximum velocity with thicker LBE film under the higher flow rate condition (see

Fig. 6). Therefore, a rounded back wall design was suggested.

Table 2. Design parameters evaluation cases

Case	Boundary Condition	Design Parameters							Results of LBE hydraulic properties		
	Inlet flow rate [GPM]	t_0 [cm]	α [°]	R_1 [cm]	L [cm]	β [°]	R_2 [cm]	γ [°]	Pressure Sign	Maximum velocity [m/s]	Film thickness @ e-beam center [cm]
1	20	3	1	5	10	40	5	5	Positive	1.95	2.1
2	30									2.25	2.4
3	20	3	5	5	10	40	5	5		1.96	2.1
4	30	4	1	5	10	40	5	5		2.08	3.1
5	32	4	1	9	1	60	5	5		2.07	3.3
6	32	4	1	9	1	60	21	-5		2.07	3.3
7	20	3	-5	5	10	40	5	5	Negative	1.94	2.1

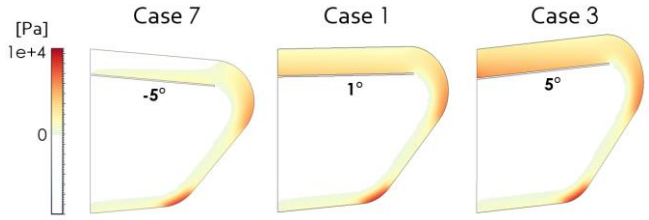

Figure 5. Effect of inlet slope on LBE pressure distribution.

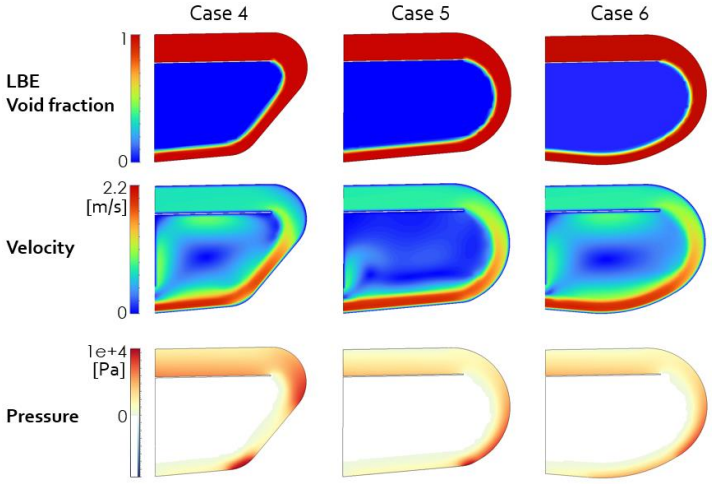

Figure 6. LBE void fraction, velocity, and pressure distribution for Case 4, Case 5, and Case 6.

Fig. 7 shows 3-D modeling results for the final converter design proposed by Niowave with a rounded back wall. The inlet channel was designed to have a decreasing channel height to hold positive pressure.

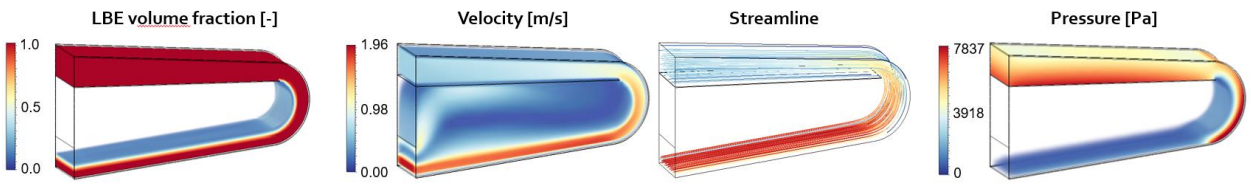

Figure 7. 3D hydraulic analysis for the final converter design.

The hydraulic analysis shows uniform and stable LBE layer formed with a maximum velocity of 1.96 m/s with a favorable pressure gradient avoiding wall separation. Positive pressure over the LBE volume assures no cavitation in LBE flow near ultra-high vacuum conditions. A mid-plane outline of the LBE profile where LBE volume fraction is greater than 0.9 was exported by point cloud data, as shown in Fig. 8. The LBE 3D volume was reconstructed in SolidWorks based on the point cloud data. The discrete geometries of LBE, Vacuum, and SS housing were then exported for radiation transport calculation described in the following section.

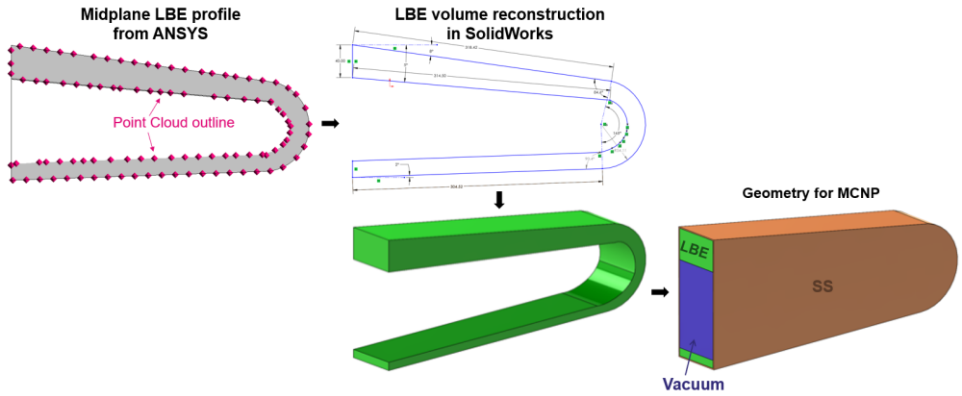

Figure 8. LBE free-surface profile extraction from CFD and LBE volume reconstruction in SolidWorks.

3 3D Radiation transport calculation

3.1 Attila4MC unstructured meshing

Volumetric heat deposition by an electron beam on the LBE converter was calculated using MCNP 6.2 code. Attila4MC developed by Silver Fir Software was used to import a customized SolidWorks geometry and to generate unstructured meshing (UM) for MCNP. The UM scheme has advantages compared to conventional constructive solid geometry (CSG) modeling scheme in several aspects. First, the UM scheme facilitates importing complex, nontrivial geometry directly from computer aided design (CAD) models. Compared to CSG modeling where users typically obtain averaged/integrated values per each cell CSG or per manually discretized mesh tallies (e.g., cmesh, tmesh), the UM scheme enables users to obtain high-resolution data per each mesh element. This capability enhances accuracy and fidelity of radiation transport calculation, especially for thin geometries. Also, the UM scheme facilitates coupling MCNP with commercial CFD tools, which are, in many cases, operating under finite element or finite volume methods (i.e., meshed scheme). The direct mapping of data from MCNP to CFD enables high-resolution 3D multiphysics analysis.

Fig.9 shows unstructured mesh generated on different sections of geometry (left) with different mesh resolution (right). To generate high-resolution mesh on 0.06 inch (~1.5 mm) thick SS plate without significantly increasing the total number of mesh elements, the geometry was subdivided into separate

regions as shown in Fig. 9. Evaluations for different mesh size were conducted, as tabulated in Table 3. LBE and SS maximum temperature was computed in ANSYS Fluent using a single mesh element size of 2 mm. Hexahedral mesh was used for LBE and tetrahedral mesh was used for SS in CFD. LBE maximum temperature varies by ~4 ℃ depending on MCNP mesh size of 2 mm or 1 mm, whereas SS maximum temperature varies by ~34 ℃. LBE maximum temperatue is less sensitivie to mesh size. When mesh is further refined to 0.6 mm, difference in SS maximum temperature reduces to ~0.6 ℃, which indicates that the solution is mesh independent. A refined mesh is required for SS plate to prevent mesh overlapping issues and to capture accurate peak temperature. Considering the convergence of data and computational costs, case 4 (LBE 2 mm, SS 0.6 mm) was selected for the rest of analyses described in the following sections.

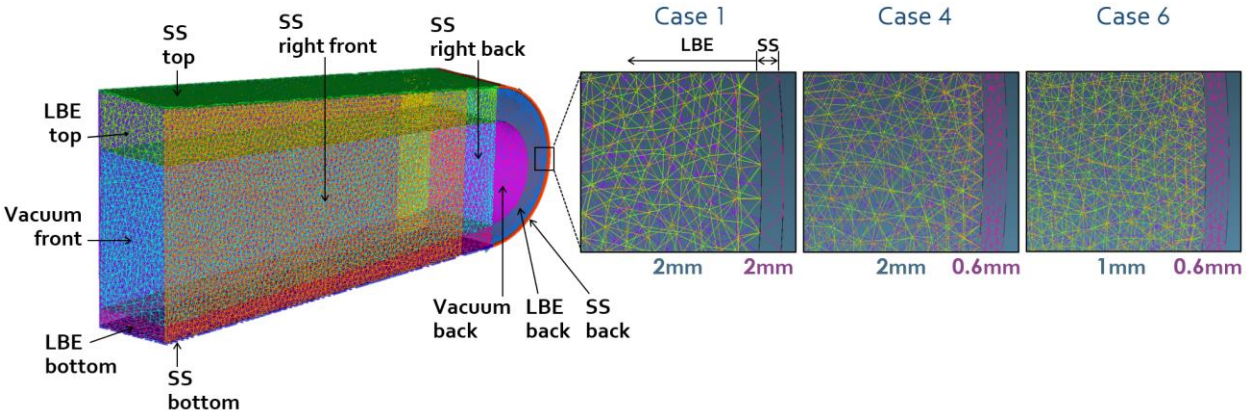

Figure 9. Unstructured meshing for the LBE converter. Mesh size was adjusted at different sectors of geometry (left) and with different spatial resolution (right).

Table 3. Attila4MC mesh size sensitivity studies

Region Name	Attila4MC Mesh Maximum Edge Length [m]					
	Case 1	Case 2	Case 3	Case 4	Case 5	Case 6
Number of elements	2,817,398	2,111,767	377,315	2,073,929	1,099,859	2,541,420
LBE heat deposition	190,954 W	194,005 W	195,561 W	193,097 W	199.268 W	199,515 W
SS heat deposition	2,898 W	3,637 W	2,942 W	3,760 W	2,718 W	3,650 W
LBE maximum temperature	**366** ℃	**363.7** ℃	**363.7** ℃	**363.2** ℃	**367.6** ℃	**367.6** ℃
SS maximum temperature	**385** ℃	**420.8** ℃	**386.5** ℃	**421.4** ℃	**383.1** ℃	**418.6** ℃
Vacuum front	0.002	0.002	0.01	0.01	0.01	0.01
Vacuum back	0.002	0.002	0.002	0.002	0.002	0.002
LBE top	0.002	0.01	0.01	0.01	0.01	0.01
LBE back	**0.002**	**0.002**	**0.002**	**0.002**	**0.001**	**0.001**
LBE bottom	0.002	0.01	0.01	0.01	0.01	0.01
SS top	0.002	0.01	0.01	0.01	0.01	0.01
SS back	**0.002**	**0.001**	**0.002**	**0.0006**	**0.002**	**0.0006**
SS bottom	0.002	0.01	0.01	0.01	0.01	0.01
SS right front	0.002	0.01	0.01	0.01	0.01	0.01
SS right back	0.002	0.002	0.002	0.002	0.002	0.002
SS left front	0.002	0.01	0.01	0.01	0.01	0.01
SS left back	0.002	0.002	0.002	0.002	0.002	0.002

3.2 MCNP calculation

An MCNP input deck was prepared for each case. The physics, material, and source terms were manually modified after packaging the input deck in Attia4MC since the software does not support electron transport. Photonuclear physics model was enabled. The electron beam has an energy of 40 MeV with 5 cm-by-5 cm cross-sectional area bounded by a cookie-cutter cell (ccc) card. Figure 10 shows MCNP results visualized using Attila4MC. Electron flux shows clear straight path of electron beam and square cross section of 5 cm-by-5 cm beam size. The converter width is 6.2 cm. Electrons mostly interact with the LBE front, then photons (i.e., bremsstrahlung) are produced by the high-energy electron interacted with the LBE atomic nuclei. Such high-energy photons knock out neutrons by photonuclear reaction such that the neutron flux and energy deposition by neutrons are mostly concentrated towards the LBE back and SS back wall. The 3D total energy deposition profile was exported as spreadsheet data and imported to CFD as point cloud heat source, as shown in Fig. 11.

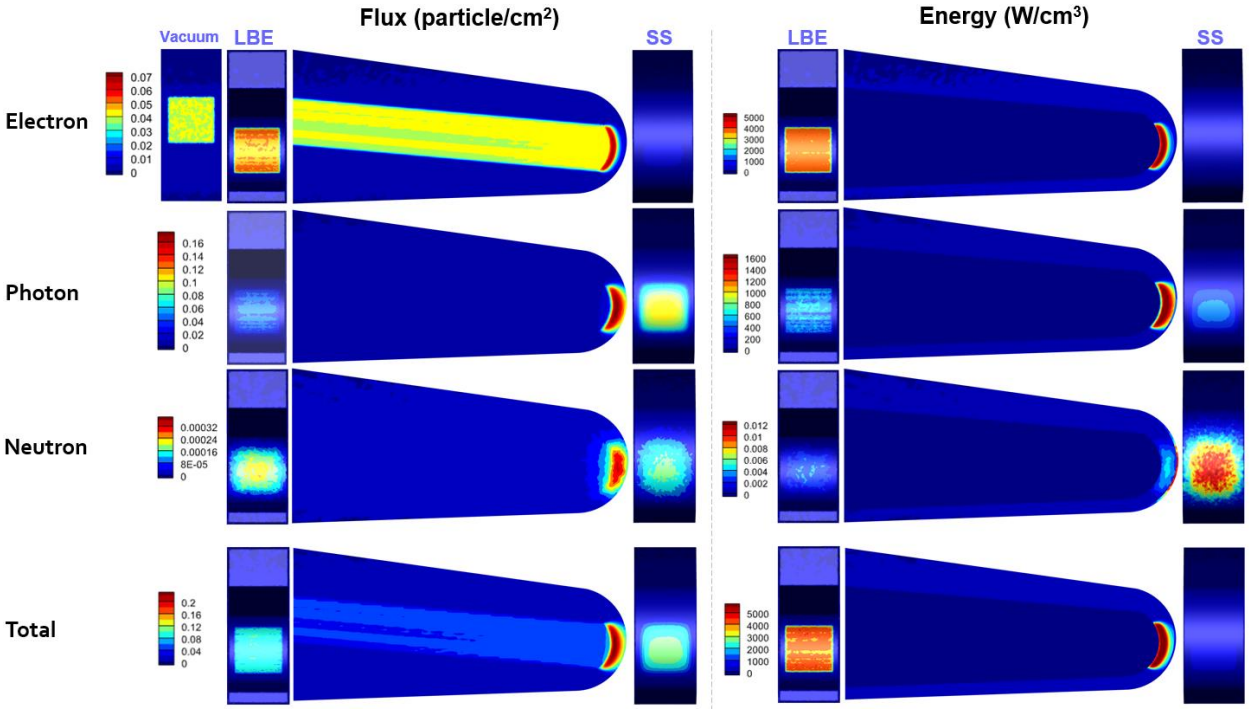

Figure 10. MCNP results: particle fluxes (left) and volumetric energy deposition (right).

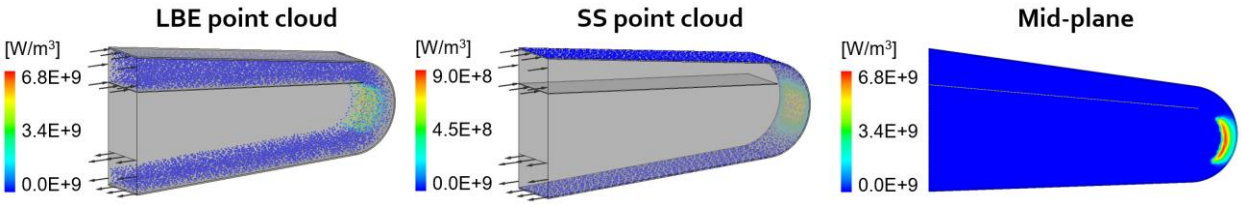

Figure 11. MCNP 3D total volumetric heating profile input to CFD as point cloud sources

4 Conjugate heat transfer (CHT) analysis

4.1 CFD mesh sensitivity studies

MultiZone – Hex mapped mesh was used for LBE. SS geometry was divided into top, bottom, right, left, and back plates, as shown in Fig. 12, to facilitate creation of hexahedral mesh, which can provide good accuracy with less computational costs compared to tetrahedral mesh. MultiZone – Hex mapped mesh was used for side (right, left) plates, and sweep mesh was used for top, back, and bottom plates. The "diving board" at the LBE inlet, shown in Fig. 12, was excluded from analysis to prevent bad mesh connection to the side (right, left) plates and bad quality mesh element creation on such thin (0.03 inch-thick) structure. Table 4 summarizes mesh statistics for 6 CFD mesh sensitivity study cases. Bulk LBE element size of 2mm with biased 0.5 mm mesh on the LBE-SS interface (Case 5) and biased 0.5 mm mesh on the LBE-SS interface plus 2 mm-thick inflation layer with uniform 0.1 mm elements (i.e., growth rate of 1) (Case 6) were used to refine the mesh near the LBE-SS interface down to submillimeter scale while minimizing increment in the total number of meshing elements.

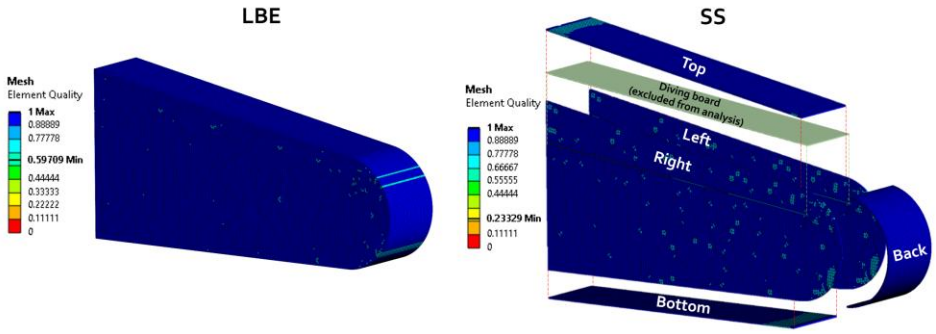

Figure 12. Hexahedral mesh on LBE and SS. Example demonstration for 2 mm uniform size.

Table 4. Mesh statistics for CFD mesh size sensitivity studies

Mesh Element Size Sensitivity Study						
	Case 1 4 mm	**Case 2** 3 mm	**Case 3** 2 mm	**Case 4** 1 mm	**Case 5** 0.5 mm*	**Case 6** 0.1 mm**
Total number of elements	54,572	121,266	385,307	3,044,748	2,554,462	5,663,800
Average element quality for LBE	0.66±0.34	0.79±0.21	0.80±0.20	0.82±0.18	0.65±0.35	0.53±0.47
Average element quality for SS back	0.36±0.23	0.56±0.19	0.93±0.03	0.95±0.02	0.73±0.24	0.28±0.11
Average aspect ratio for LBE	3.07±2.06	2.49±1.49	1.94±0.94	1.59±0.59	3.62±2.62	11.31±10.30
Average aspect ratio for SS back	3.59±2.05	1.82±0.37	1.28±0.06	1.3±0.08	2.14±0.90	5.18±0.27
Average orthogonal quality for LBE	0.79±0.20	0.84±0.16	0.87±0.13	0.89±0.11	0.87±0.13	0.60±0.40
Average orthogonal quality for SS back	0.59±0.39	0.71±0.29	0.97±0.03	0.98±0.02	0.90±0.10	0.97±0.02

* SS 0.5 mm. LBE-SS interface surface 0.5 mm with biased mesh towards bulk LBE element 2 mm.
** SS 0.1 mm biased mesh through thickness direction. LBE 2 mm (bulk)—0.5 mm (LBE-SS interface) biased mesh with 2 mm thickness inflation layer with 0.1 mm uniform element.

Fig. 13 shows mid-plane temperature profiles with mesh lines and border lines of LBE volume fraction greater than 0.9 and SS. Line profiles of LBE volume fraction, velocity, pressure, and temperature along line 1 and line 2 for Case 1-6 are shown in Fig. 14. Line 1 locates at the center of the beam, and line 2 locates at the edge of the beam. The line profiles of thermohydraulic properties converged with mesh refinement down to 1 mm. Table 5 summarizes the maximum temperature at LBE, SS, LBE-SS interface, and outlet, at line 1 and line 2, for cases 1-6. Fig. 15 shows the maximum temperature as a function of number of mesh elements, which converged after the number of elements reached above 2,000,000.

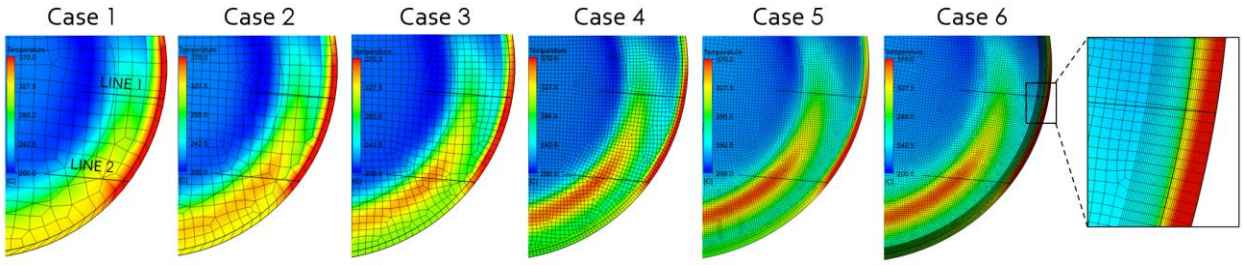

Figure 13. Mid-plane temperature profile with mesh lines and border lines for LBE and SS.

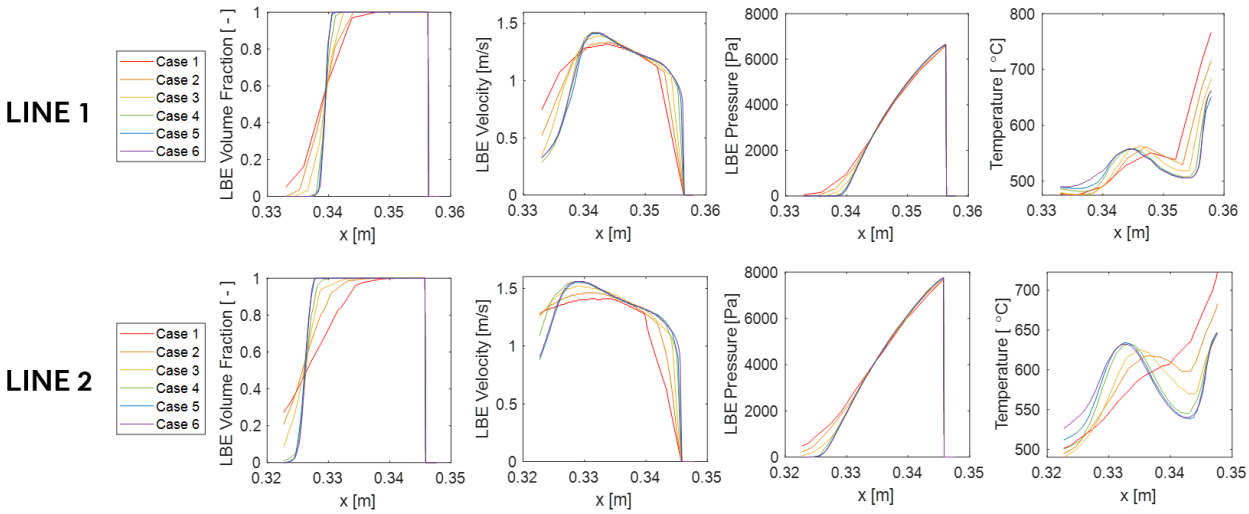

Figure 14. Line profiles of thermohydraulic properties at line 1 and line 2.

Table 5. Maximum temperature

Mesh Element Size Sensitivity Study Cases						
	Case 1 4 mm	**Case 2** 3 mm	**Case 3** 2 mm	**Case 4** 1 mm	**Case 5** 0.5 mm*	**Case 6** 0.1 mm**
LBE	339.8 ℃	352.8 ℃	359 ℃	363.1 ℃	363.6 ℃	362.6 ℃
SS	526.9 ℃	459.2 ℃	422 ℃	413.8 ℃	409.4 ℃	407.7 ℃
Interface @ LINE 1	443.8 ℃	397.8 ℃	363.8 ℃	330.8 ℃	304.8 ℃	307.8 ℃
Interface @ LINE 2	413.8 ℃	379.8 ℃	346.8 ℃	345.8 ℃	339.8 ℃	339.8 ℃
Outlet	321 ℃	330 ℃	322 ℃	327.4	319.8 ℃	326.7 ℃

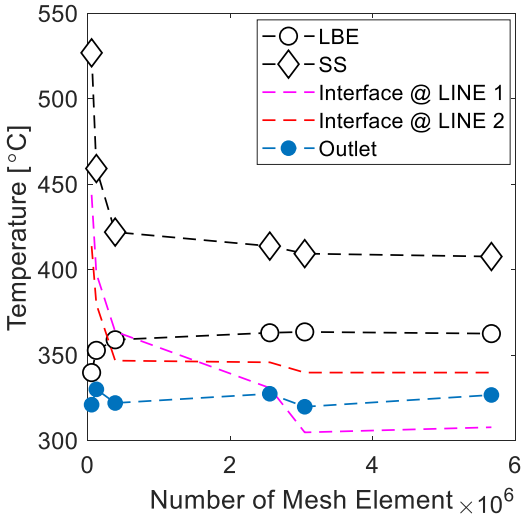

Figure 15. Maximum temperature as a function of number of mesh elements

4.2 CHT analysis results

Based on MCNP and CFD mesh sensitivity studies, final conjugate heat transfer (CHT) analysis was performed with MCNP unstructured mesh size of LBE 2 mm – SS 0.6 mm, and CFD structured mesh size of 1 mm. Fig. 16 shows the 3D temperature profile at LBE (left top), 2D temperature profiles at LBE-SS interface, SS back wall, and mid-plane (left bottom), and temperature line profiles at line 1 and line 2 (right). The calculated thermohydraulic properties are summarized in Table 6. LBE maximum temperature reaches 363 ℃, below the LBE evaporation initiative temperature, 450 ℃. LBE-SS interface temperature at line 2 is 346 ℃, which has low risk of severe SS corrosion problem.

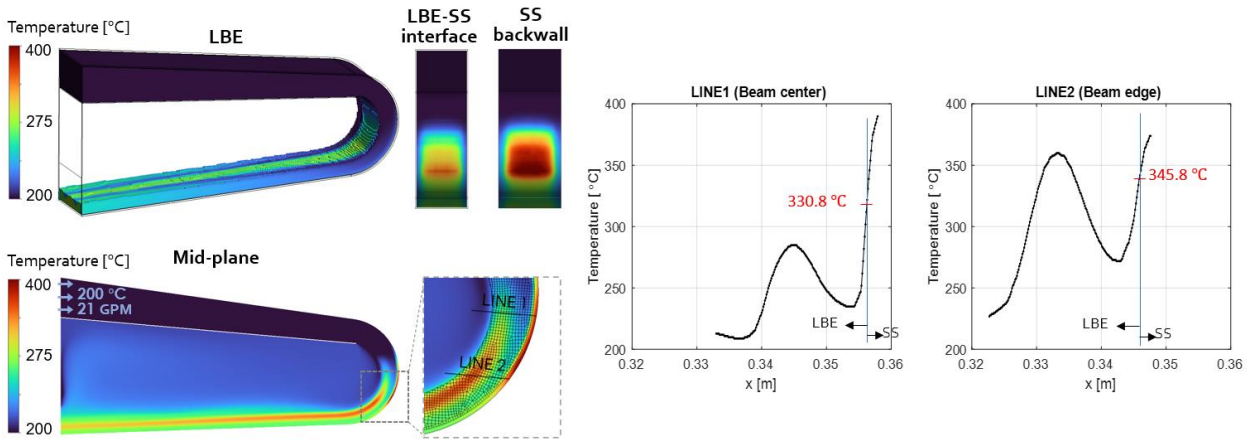

Figure 16. Temperature profiles for LBE and SS

Table 6. Final CHT analysis results.

Thermohydraulic Properties	
LBE centerline thickness	1.6 cm
LBE heat deposition	172,134 W
SS back heat deposition	3983 W
LBE maximum temperature	363 ℃
SS back maximum temperature	414 ℃
Interface temperature @ Line 1	331 ℃
Interface temperature @ Line 2	346 ℃
Outlet maximum temperature	327.4 ℃
Maximum LBE velocity	1.84 m/s
Maximum LBE pressure	8220 Pa

5 Conclusions

LANL have evaluated Niowave's LBE windowless target, neutron source converter design using multiphysics analysis. Discrete LBE, SS, vacuum geometries were created in SolidWorks based on 3D CFD hydraulic simulation, then imported to Attila4MC. Through unstructured mesh size sensitivity studies, 2 mm mesh for LBE and 0.6 mm mesh for SS were selected for MCNP analysis. The total volumetric heat deposition 3D profile was imported to CFD to conduct CHT analysis. CFD structured mesh sensitivity studies showed converged results when mesh element size is as small as 1 mm and the total number of elements is larger than 2,000,000. The final results demonstrated that LBE film has centerline thickness of 1.6 cm with the maximum velocity of 1.84 m/s, which is under velocity limitation of 2 m/s to prevent LBE-SS interface erosion issues. Maximum temperature of LBE, SS, and LBE-SS is 363 ℃, 450 ℃, and 346 ℃, respectively, of which all values satisfy the thermal safety limitation to prevent LBE evaporation and severe corrosion on LBE-SS interface. By virtue of LANL's coupled radiation transport and thermohydraulic analyses, Niowave can proceed to build the experimental LBE loop facilities to test the neutron converter design.

6 Continuation of work in FY24

6.1 Design and analysis of a 200 kW converter

The design and analysis of a 200 kW converter will be continued in FY24 as the system evolves. Niowave had made modifications to three components after the aforementioned multiphysics analyses were done: the length of the converter is extended, the inlet introduces LBE into the converter by merging flow from two pipes, and the outlet piping is curved to be designed following free-stream LBE flow, as shown in Fig.17 (left). The LBE flow rate is also increased from 21 GPM to 25 GPM.
Preliminary study has been initiated for hydraulic-only analysis of the fluid domain. Tetrahedral and hexahedral meshes were combinedly used for the inlet and outlet piping with varying element size of 2mm-4mm (see Fig. 17 right). Overall mesh statistics and metric are summarized in Table 7.

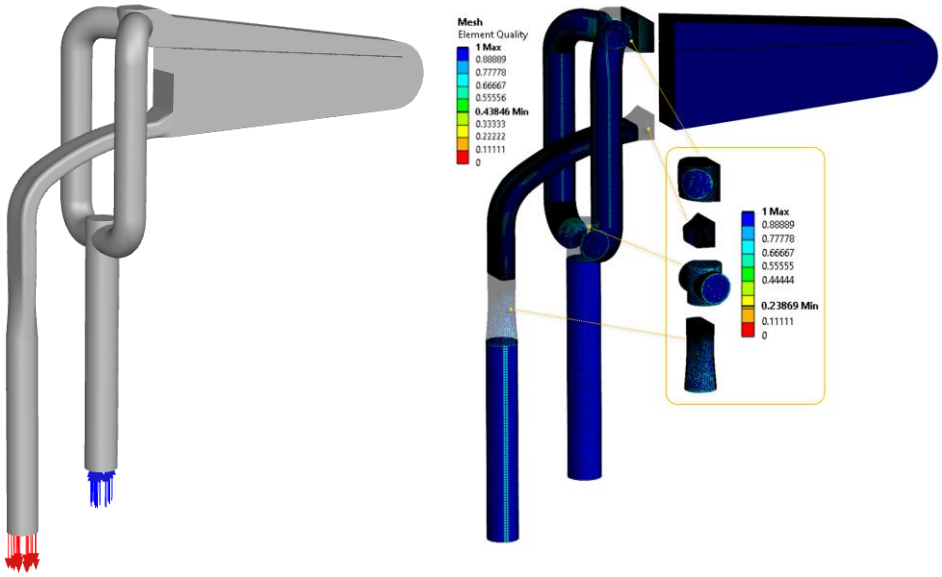

Figure 17. Modified converter design (left) and meshing for the preliminary study (right).

Table 7. Overall mesh statistics and metric

Total number	
Elements	5291313
Nodes	4671997
Element Quality	
Maximum, Minimum, Average	1, 0.2416, 0.96216
Number of elements below 0.5	7082
Aspect Ratio	
Maximum, Minimum	9.4945, 1
Orthogonal Quality	
Maximum, Minimum	1, 0.10748
Skewness	
Maximum, Minimum	0.89252, 1.6719E-8

The upstream merged piping induces unsteady, chaotic flow at the inlet, as shown in Fig. 18. Hydraulic simulations are running to check such turbulent behavior and the pressure/velocity field distribution. Significant backflow has been observed at the outlet in computational solutions with two different time steps, 0.1s and 0.001s, as shown in Fig. 19. Below options are available to overcome such numerical/physical issues:

- Decrease the order of magnitude of time step, e.g., 0.0001s.
- Step increase the flow rate, e.g., start with 3 GPM→ solution converged → increase to 7 GPM ..
- Change boundary conditions, e.g., pressure inlet and mass flow rate outlet for better robustness.
- Change outlet geometry, e.g., elongated parallel line to replicate actual production system.

CFD hydraulic analysis will continue and be used to inform revisions to the inlet/outlet pipe design, if necessary. MCNP-coupled multiphysics CTH analysis can be also continued in FY24 for the updated design.

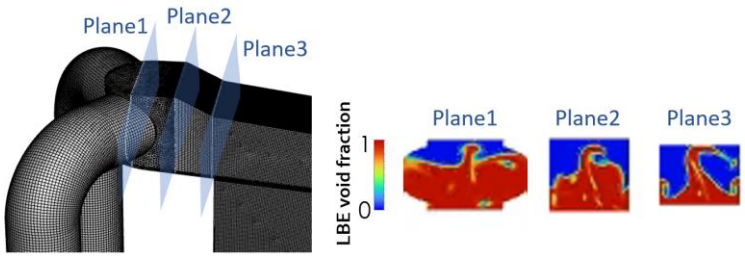

Figure 18. Transient LBE void fraction in three cross-sectional views.

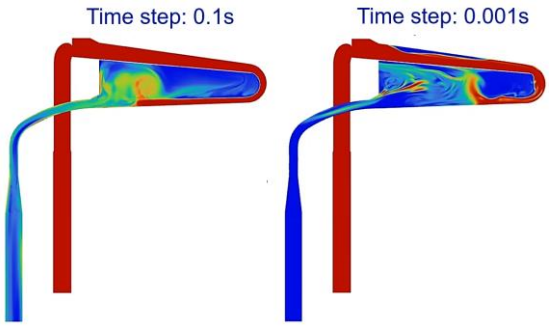

Figure 19. Significant backflow for the modified inlet/outlet design.

6.2 200 kW heat exchanger design and analysis

A heat exchanger (HX) enables LBE to maintain a stable supply temperature of 200 ℃ to a converter by removing heat via water pool boiling. The design previously tested at low power (10 kW), preferred by Niowave, is with the 2° downward-tilt LBE pipe surrounded by a shell of a partially filled static water pipe, with water supply rate matching the evaporation rate, as shown in Fig. 20.

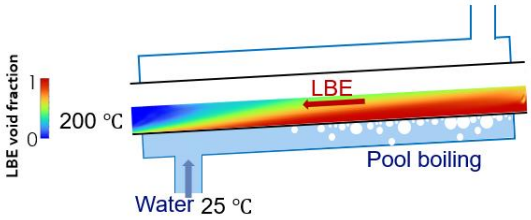

Figure 20. Conceptual design of a heat exchanger.

A preliminary numerical study has been conducted for a 4m-long HX. HX domain was segmented into 0.1m-long sections, as shown in Fig. 21, where $T_{LBE,i}$ is bulk LBE temperature at node i, $T_{SS,in,i}$ is SS pipe inner surface (which is in contact with LBE) temperature, $T_{SS,out,i}$ is SS pipe outer surface (which is in contact with water) temperature, and $A_{H,i}$ is heat transfer area where pipe areas covered by LBE and water are overlapped. LBE cross-sectional area at node i, A_i, can be calculated by continuity (Eq. 1) and Bernoulli's (Eq.2) equations:

$$v_i A_i = v_{i-1} A_{i-1} \tag{1}$$

where v_i is LBE velocity $[m/s]$ at node i.

$$\frac{\rho v_i^2}{2} = \frac{\rho v_{i-1}^2}{2} + \rho g(0.1 \sin(2°)\,[m]) \tag{2}$$

where ρ is LBE density (used constant value for hydraulic analysis) $[kg/m^3]$ and g is gravitational acceleration $[m/s^2]$.

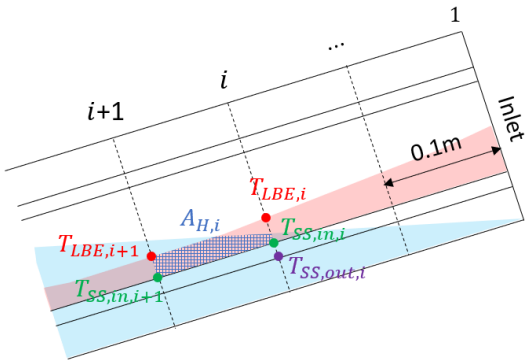

Figure 21. Schematic diagram of discretization.

Inlet boundary conditions were given by CFD, postulating a short rectangle-to-round adapter connecting the converter outlet (i.e. simulation results in Section 2 and 4) with the HX inlet, as shown in Fig. 22. Quantities averaged over area where LBE volume fraction is larger than 0.9 were used as inlet conditions for the numerical study, as summarized in Table 8.

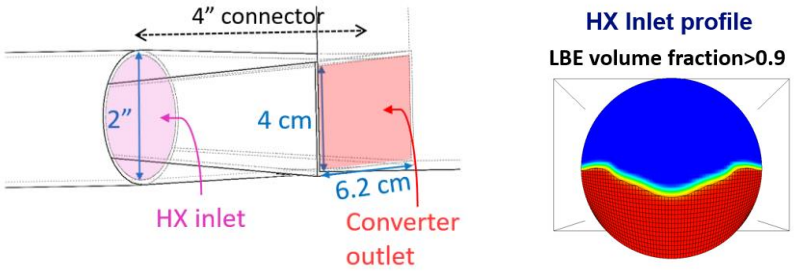

Figure 22. HX inlet LBE profile given by CFD.

Table 8. HX inlet conditions.

Area-averaged LBE thermohydraulic Properties	
LBE effective area (A_1)	0.00071558 m^2
Velocity (v_1)	1.697 m/s
Density (ρ_1)	1.338.3 kg/m^3
Mass flow rate ($\dot{m}$)	12.5554 kg/s
Temperature ($T_{LBE,1}$)	288.876 ℃

Heat transfer area along a HX longitudinal direction is shown in Fig. 23.

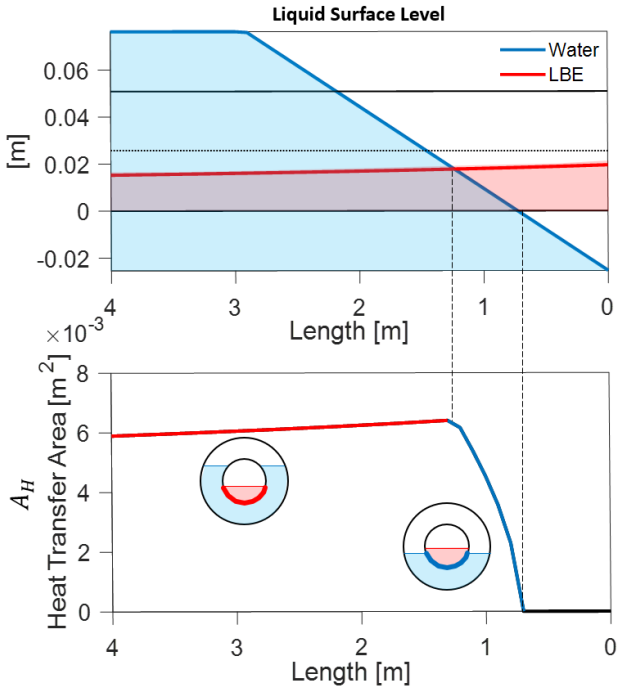

Figure 23. Liquid surface level and corresponding heat transfer area.

For heat transfer analysis, linear/polynomial fitting functions for material properties of LBE and SS in Fig. 3 and Fig. 4 were used. Empirical correlations for LBE-side heat transfer coefficient (HTC), h_{LBE} (see Eq. 3), and water-side nucleate boiling HTC, h_{NB} (see Eq. 4), were used. However, HTC should be systematically investigated in future study for higher accuracy and reliability.

$$h_{LBE} = \frac{Nu \cdot k}{D_h},\ Nu = 4.5 + 0.018Pe^{0.8}\ [2],\ D_h = \frac{4A}{P_w} \tag{3}$$

where k is LBE thermal conductivity $[W/(mK)]$, Nu is Nusselt number for LBE, D_h is LBE hydraulic diameter $[m]$, Pe is Péclet number for LBE, A is LBE cross-sectional area $[m^2]$, and P_w is wetted perimeter $[m]$.

$$h_{NB} = \frac{q}{(T_s - T_b)},\ q" = \mu h_{fg}\left(\frac{g(\rho_L - \rho_v)}{\sigma}\right)^{1/2}\left(\frac{c_p(T_s - T_{sat})}{C_{sf}h_{fg}Pr}\right)^3\ [3] \tag{4}$$

where T_s is surface temperature $[K]$, T_b is bulk water temperature $[K]$, $q"$ is heat flux $[W/m^2]$, μ is water dynamic viscosity $[kg/(ms)]$, h_{fg} is water latent heat of evaporation $[J/kg]$, ρ_L is liquid water density $[kg/m^3]$, ρ_v is vapor density $[kg/m^3]$, σ is surface tension for liquid-vapor interface $[N/m]$, c_p is water specific heat $[J/(kgK)]$, T_{sat} is saturation temperature, C_{sf} is surface-fluid factor, where the value of 0.013 has been widely investigated among water-metal data [3], and Pr is Prandtl number for liquid water. Since both heat flux and SS surface temperature are unknown, solutions were obtained via an iterative method as follows:

Step 1: Guess initial value of $T_{SS,out,i}$.

Step 2: Calculate $q"_i$ using Eq. 2.

Step 3: Calculate $T_{LBE,i} = \frac{q"_i A_{H,i}}{\dot{m} c_{p,i}}$, where $\dot{m}$ is LBE mass flow rate $[kg/s]$ given as an inlet boundary condition and $c_{p,i}$ is LBE specific heat at $T_{LBE,i-1}$(explicit).

Step 4: Calculate $T_{SS,in,i} = T_{LBE,i} - \frac{q"_i}{h_{LBE.i}}$ with known value of $h_{LBE.i}$ obtained using Eq. 1.

Step 5: Calculate $T_{SS,out,i} = T_{SS,in,i} - \frac{q"\delta}{k_{SS,i}}$, where δ is SS wall thickness (0.065") and $k_{SS,i}$ is SS thermal conductivity at $T_{SS,in,i-1}$ (explicit). If $T_{SS,out,i}$ is different from the initial guess, update $T_{SS,out,i}$ value and iterate STEP 1~5.

LBE and SS wall temperature, heat flux, and LBE and SS HTCs along a HX longitudinal direction are shown in Fig. 24.

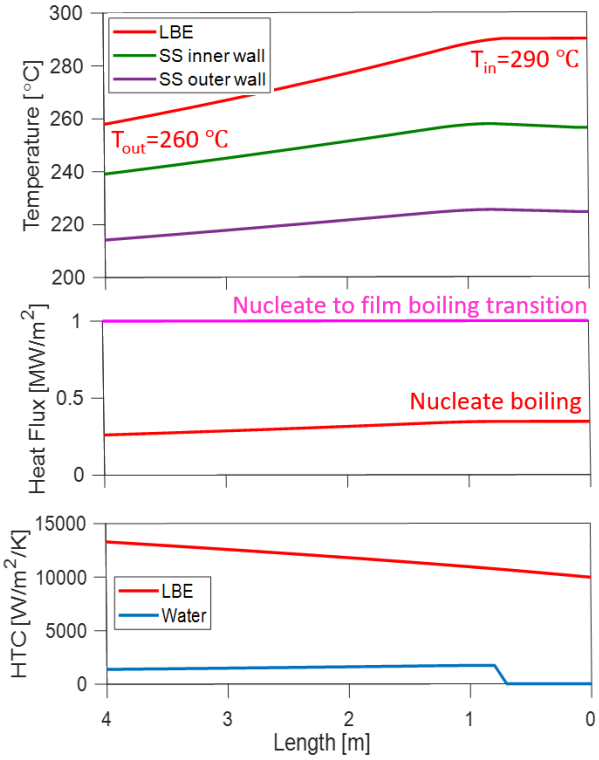

Figure 24. Temperature, heat flux, and heat transfer coefficient along the HX length.

The result shows that 4m length is not enough to cool LBE temperature down to 200 ℃. Alternatively, a heat exchanger can be placed on the LBE supply side, as a completely full pipe of the vertical arrangement. Variations on location and configuration will be analyzed in FY24. For example, a multiple tube configuration may be practical, similar to a shell and tube heat exchanger design. Analytical and computational analyses will be conducted, with systematic investigation about HTCs and pool boiling bubble dynamics CFD models.

7 References

[1] K. Woloshun, E. Olivas, C. Miera, T. Roybal, B. Singh, “Niowave design and analysis of a 200 kW converter,” *Los Alamos National Lab.* 2022. LA-UR-22-28049

[2] X. Cheng, N. Tak, “Investigation on turbulent heat transfer to lead-bismuth eutectic flows in circular tubes for nuclear applications,” *Nucl. Eng. Des.* 2006, 236 (4) 385-393.

[3] W. N. Rohsenow, “A method of correlating heat-transfer data for surface boiling of liquids,” *Trans. ASME.* 1952, 74 (6) 969-975.